A NEW APPROACH IN SINTERING FORMULATIONOF A CRYSTALLINE POLYMER FOR SELECTIVE LASER SINTERING APPLICATION

Alva E. Tontowi

The Industrial Engineering, the Department of Mechanical Engineering-UGM
E-mail: menaet@yahoo.com
http://www.geocities.com/menaet

ABSTRACT

This paper reports the results of an investigation in sintering formulation of a crystalline polymer. It highlights a development of a new approach to formulation of a sintering process based on the viscosity measurement due to the lack of crystalline polymer's data. Two areas were addressed during the investigation: viscosity of melting and sintering formulation based on the viscosity results. A nylon-12 based material powder was used both in the model and experiment. To examine this new formula, test case was carried out to predict activation energy and pre-exponential factor and ultimately to predict sintered part density of a crystalline polymer. The results show that sintering formula for crystalline polymer can be developed on the basis of the amorphous polymer data. The density's prediction gives a good agreement with the measurement for the activation energy (E_s/R) of 12266.78 K and pre-exponential factor (A_s) of 50E+10 s^{-1}.

Keywords: amorphous, crystalline, viscosity, activation energy, sintering, density.

1. INTRODUCTION

Selective laser sintering is one of the rapid prototyping technologies that currently growing very fast since this technology is able to reduce processing time, cost and to build parts with geometrically very complex. As a result, product can be introduced to market faster. This technology naturally works based on the classical sintering process i.e. bonding particle using heat. A three dimensional part is made of layer by layer of sintered powder following the slices of the 3D CAD images. The process begins with drawing the 3D part using CAD's software, it is numerically sliced and converted into *.STL* file. This file is then sent to a sintering process to build a physical part. In this, the process begins with spreading powder on the bed as representing the first slice of the 3D image (typically the bottom layer). Then, the laser scans this powder layer following the first slice image. Next, fresh powder spreads over the first layer and laser scans it following the second slice image. The same process cycle continues until a 3D part is completed. Applying this technology, however, although it gives many advantages as mentioned above, building a physical part directly is very often getting risk such as low density and dimension inaccuracy due to the less or over power. As a result, not saving time will be got, but the longer time and more cost due to the process has to be repeated. For these reasons, modelling of this process that enable user to predict the density of sintered parts before building parts in the machine is very important. This paper reports an investigation in developing a new approach to formulate a sintering process of a crystalline polymer based on the viscosity measurement results.

2. SINTERING MODEL

A two dimensional sintering model was developed on the basis of a typical conduction heat transfer equation and sintering law for amorphous polymer. To support the model, experimental work

has been carried out only for viscosity as this data was not available yet. Other data are obtained from other publications.

2.1. Conduction heat transfer equation

As shown in equation (1), the right side of this equation, the three parts show an initial thermal conductivity k and it varies with temperature and position, the fourth part (V) shows a powder bed is moving relatively to the heat source (i.e. laser beam), and the last part (L) shows a latent heat for melting as the material is crystalline polymer.

$$\rho C\frac{\partial T}{\partial t}=k\left(\frac{\partial^2 T}{\partial y^2}+\frac{\partial^2 T}{\partial z^2}\right)+\frac{\partial k}{\partial T}\left\{\left(\frac{\partial T}{\partial y}\right)^2+\left(\frac{\partial T}{\partial z}\right)^2\right\}+\left(\frac{\partial k}{\partial y}\frac{\partial T}{\partial y}\right)+\left(\frac{\partial k}{\partial z}\frac{\partial T}{\partial z}\right)-\rho CV\frac{\partial T}{\partial y}+\rho L\frac{\partial \alpha}{\partial t} \quad (1)$$

where ρ is density, C is specific heat, V is velocity, k is thermal conductivity, L is the latent heat, α is the solid fraction, T is temperature and (y, z) is the position.

2.2. Existing sintering law and densification (amorphous polymer)

The existing sintering law for amorphous polymer assumes thermally activated viscous sintering (Childs *et al*, 1997).

$$f=A_s e^{\frac{-E_s}{RT}} \quad (1)$$

and density is assumed to vary with time as equation (2).

$$\frac{d\rho}{dt}=(\rho_{\max}-\rho)A_s e^{\frac{E_s}{RT}} \quad (2)$$

2.3. A new approach of sintering law and densification (crystalline polymer)

Following the previous model of the selective laser sintering of crystalline polymers, the sintering law proposed in this work has been developed and to fit experimental observations. It is supposed that viscous sintering remains the mechanism, so that in the expression for void elimination rate

$$\frac{d\varepsilon}{dt}=-f\varepsilon \quad (3)$$

f remains dependent on surface tension σ, viscosity η and particle shape and size (radius a):

$$f\propto\frac{\sigma}{\eta}=c_s\frac{\sigma}{\eta} \quad (4)$$

where c_s is a constant for any powder, being a function of powder shape and size.

There are two developments in this section. Firstly, it is considered how η for a melting crystalline polymer and a melting crystalline polymer, differs from η of an amorphous polymer. Secondly, it is considered how equation (4) can be used to obtain f for a particular polymer, without carrying out sintering experiments.

a. Viscous behaviour of crystalline polymers

A melting polymer containing amorphous and crystalline parts has a viscosity that can be formulated as follows (Ziabicki *et al*, 1993)

$$\eta(T,X)=\eta_{melt}(T)\eta_x(X) \quad (5)$$

Viscosity of the amorphous part η_{melt} is assumed to follow the Arrhenius equation, and is given by

$$\eta_{melt}(T)=A_\eta e^{\left(\frac{E_\eta}{RT}\right)} \quad (6)$$

and the viscosity of the crystalline part η_x is given by (Shimizu *et al*, 1985)

$$\eta_x(X)=e^{(a_x X^b)} \quad (7)$$

Substitution of equation (6) and (7) into equation (5)

$$\eta(T,X)=A_\eta e^{\left(\frac{E_\eta}{RT}\right)}e^{(a_x X^b)} \quad (8)$$

or in another form

$$\eta(T,X)=A_\eta e^{\left(\frac{E_\eta}{RT}+a_x X^b\right)} \quad (9)$$

where A_η is the pre-exponential factor of viscosity, E_η is the activation energy of viscosity, R is the gas constant, T is temperature, a_x and b are crystalline constants, and X is the crystalline fraction.

During melting the phase changes from solid to liquid, the ordered molecules of the crystalline polymers are broken down to become random like an amorphous polymer. The crystalline fraction (X) reduces from 1 to 0 (in many polymers, the crystalline fraction in the solid state is less than 1, but here this is ignored). In other words, the crystalline content reduces from 100 % to nothing. Based on the similarity of the phase change to the crystalline fraction evolution, the change of X is the same

as the change of α Equation (9) then becomes

$$\eta(T,\alpha) = A_\eta e^{\left(\frac{E_\eta}{RT}+a_x\alpha^b\right)} \quad (10)$$

b. Development of sintering law and densification

Following Frenkel (1945) and Mackenzie and Shuttleworth (1949) on viscous flow that, sintering rate is directly proportional to the surface tension s and inversely proportional to the viscosity η, it is assumed here that sintering rate of crystalline polymers is also given by

$$f = c_s \frac{\sigma}{\eta(T,\alpha)} \quad (11)$$

Adapting equation (1) with a crystalline term, sintering rate then can also be written as

$$f = A_s e^{\left(\frac{-E_s}{RT}-a_x\alpha^b\right)} \quad (12)$$

and densification in equation (2) becomes

$$\frac{d\rho}{dt} = (\rho_{max} - \rho)A_s e^{\left(\frac{-E_s}{RT}-a_x\alpha^b\right)} \quad (13)$$

Once a crystalline polymer is fully molten (α=0), this treatment implies there is no difference in sintering behaviour between a crystalline and an amorphous polymer. Then combination of equation (11) and (12) gives equations which may be used to predict activation energy and pre-exponential factor for sintering of crystalline and composite polymers from knowledge of the behaviour of amorphous polymers.

$$\left[\frac{A_s e^{\left(\frac{-E_s}{RT}\right)} A_\eta e^{\left(\frac{-E_\eta}{RT}\right)}}{c_s\sigma}\right] = const \quad (14)$$

If we have two different polymers, one originally crystalline (identified as X) or composite crystalline (XC), the other an amorphous polymer (A), equation (14) lead to

$$\left[\frac{A_s e^{\left(\frac{-E_s}{RT}\right)} A_\eta e^{\left(\frac{E_\eta}{RT}\right)}}{c_s\sigma}\right]_X = \left[\frac{A_s e^{\left(\frac{-E_s}{RT}\right)} A_\eta e^{\left(\frac{E_\eta}{RT}\right)}}{c_s\sigma}\right]_A \quad (15)$$

If surface tension σ follows an Arrhenius law, equation (15) become (16).

$$\left[\frac{A_s e^{\left(\frac{-E_s}{RT}\right)} A_\eta e^{\left(\frac{E_\eta}{RT}\right)}}{c_s A_\sigma e^{\left(\frac{E_\sigma}{RT}\right)}}\right]_X = \left[\frac{A_s e^{\left(\frac{-E_s}{RT}\right)} A_\eta e^{\left(\frac{E_\eta}{RT}\right)}}{c_s A_\sigma e^{\left(\frac{E_\sigma}{RT}\right)}}\right]_A \quad (16)$$

Indexes $_X$, $_A$, $_{XC}$ and $_{AC}$ indicate crystalline, amorphous, crystalline composite and amorphous composite.

In the selective laser sintering literature, data on A_s, E_s, A_η, E_η and σ, exists for the amorphous polymer Polycarbonate. If viscous and surface tension data is known for the X polymer, equation 16 allows A_s and E_s to be deduced for that. In this paper, this approach is used to estimate A_s and E_s for Duraform polyamide. Because the c_s values of these materials and the standard Polycarbonate are not known, they have been assumed to be the same for all the materials. This assumption is tested by comparing predicted and observed sintering behaviour.

3. EXPERIMENT METHOD ON VISCOSITY

As mentioned in equation (4) that pre-exponential factor A_s and activation energy for sintering E_s of Duraform polyamide were deduced from the data available in polycarbonate, here experiment works were carried out only to measure viscosity of melting of this material.

3.1. Material

Material was used in this experiment is Duraform polyamide. This material is a crystalline polymer produced by DTM Corp USA. Specification of the material is shown in Table 1.

Table 1: Material data

	Crystalline polymer (Duraform polyamide)	Amorphous polymer Polycarbonate
A_η (Pa.s)	0.6103	5.63e-10 [4]
A_σ (mN/m)	17.3 [2]	20.5
A_s (1/s)	-	8840000e+10
E_η/R (K)	3031.26	15147.9 [4]
E_σ/R (K)	191.36 [2]	217.44
E_s/R (K)	-	21000.00

3.2. Equipment

Measurement of melt viscosity was carried out in the Rosand capillary rheometer shown in Figure 1. It consists of two bores with a diameter of 25 mm surrounded by a heater block, two plungers and piston tips, and two capillary dies, both with diameter of 1 mm but different lengths of 1 mm and 10 mm, respectively. The two different capillary die lengths have been used in the rheometer to correct for end-loss effects. These effects are associated with extra pressure drops at the entrance and exit of the die.

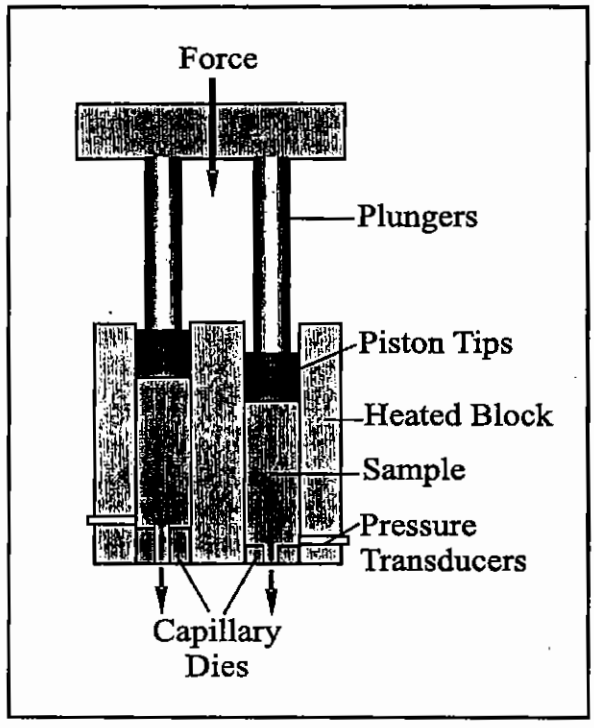

Figure 1. Schematic diagram of dual-bore capillary rheometer

3.4. Method of measurement

The method of measurement is referred to in the ASTM D-3835, Rheological Properties of Thermoplastics with a Capillary Rheometer. The rheometer piston pushes the material sample at a constant temperature and flow rate, Q, through a cylindrical die of known length, L, and diameter, d. The apparent shear rate is defined as:

$$\dot{\gamma}_a = \frac{32Q}{\pi d^3} \qquad (5)$$

By measuring the pressure drop across the die, $\Delta p = P_{Long} - P_{Short}$, the wall shear stress is calculated as:

$$\tau_w = \frac{\Delta p}{4\left(\frac{L}{d}\right)} \qquad (6)$$

and the apparent shear viscosity is calculated as

$$\eta_a = \frac{\tau_w}{\dot{\gamma}_a} \qquad (7)$$

In the experiment, the apparent shear rate was set at 100 to 5000/s for the three temperatures of 200, 220 and 240 °C. The apparent shear viscosity is expected to be equal to the melt viscosity.

$$\eta_a = \eta_{melt} \qquad (8)$$

During the process of melting, elimination of the degree of crystallinity takes place. Subsequently, all regions within the polymer can be assumed to be amorphous. In the absence of crystallinity, the viscosity can be approximated by the Arrhenius equation,

$$\eta_{melt}(T) = A_\eta \exp\left(\frac{E_\eta}{RT}\right) \qquad (9)$$

where A_η is a material constant, usually dependent on molecular weight (intrinsic viscosity) of the polymer, R is the gas constant, T is the absolute temperature and E_η is the constant activation energy for melting. In the experiment, this viscosity, $\eta_{melt}(T)$, assumed to be the apparent shear viscosity η_a, is used to determine A_η and E_η/R.

3.5. Test condition

The test conditions of the experiment are in Table 2. Shear rates stated in the Table are applied to the whole range of heating temperature for the Duraform polyamide being tested.

Table 2: Test conditions of viscosity measurement

Parameters	Materials (powder) Duraform Polyamide
Heating temperature (°C)	200, 220, 240
Shear Rate (1/sec)	100 to 5000

4. RESULTS AND DISCUSSION

4.1. Viscosity

As discussed in section 3, molten polymer viscosity measurement was carried out in the Rosand capillary rheometer. In the experimental work, only Duraform polyamide has been studied.

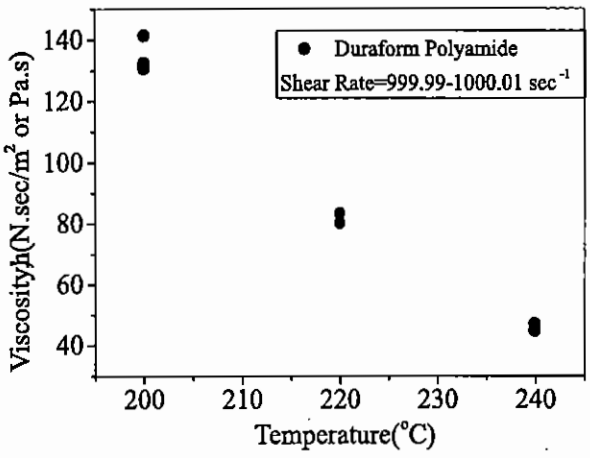

Figure 2. Shear viscosity for varying heating tem perature

In the experiment, shear rate was set in the range 100 to 5000 sec^{-1}, at temperatures of 200, 220 and 240 °C. Results of the experiment for Duraform polyamide are shown in Figure 2. These results describe the relationship between viscosity and temperature. In this case, an increase of heating temperature is followed by a decrease of the viscosity.

It was only possible, with the equipment available, to measure viscosity over the whole temperature range 200 °C to 240 °C at the shear rate of @1000 sec^{-1}. At lower shear rates, at 240 °C, the Rosand viscometer was not sensitive enough to measure viscosity, while at higher shear rates at 200 °C, the viscometer was not powerful enough. It is interesting to point out that at a heating temperature equal to or higher than 200 °C, the viscous flow type Duraform polyamide tends to be non-Newtonian.

4.2. Pre-exponential factor and activation energy of viscosity and sintering

The activation energy and pre-exponential factor for the sintering of Duraform polyamide has been obtained, following equation 4. This requires the temperature dependence of both viscosity and surface tension of the polymer to be known. The temperature dependence of viscosity comes from Section 4.1 and of surface tension from handbook data. Here viscosity temperature dependence is considered first, before surface tension and sintering rate estimates.

4.2.1. Viscosity: A_η and E_η/R

The results of Figure 2 is replotted in Figure 3 in the form of natural logarithm against the inverse of absolute temperature. A linear fitting equation of these data is written as follows

$$\ln \eta = -8.51 + 6341\left(\frac{1}{T}\right) \qquad (10)$$

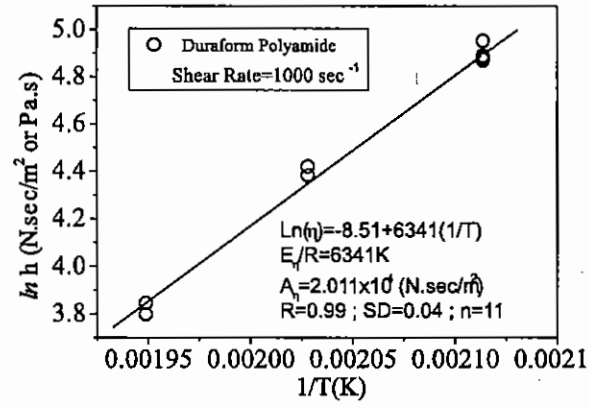

Figure 3. Natural log of viscosity against 1/T for shear rate@1000 sec^{-1}.

From equation (10), $\eta = A_\eta exp(E_\eta/RT)$, with the activation energy for Duraform polyamide, E_η=12590 J/mole or E_η/R=6341 K and the pre-exponential factor, A_η= 2.011E-04 N.sec/m^2 or Pa.s. The linear fitting has a strong correlation within the data, as it has a coefficient of correlation R=0.99, with a standard deviation of 0.04 N.sec/m^2.

4.2.2. Pre-exponential factor and activation energy for sintering: A_s and E_s/R

According to equation (4), activation energy and pre-exponential factor E_s and A_s in sintering can be obtained from E_η and A_η and the activation energy and pre-exponential factor E_σ and A_σ of surface tension. In this paper, surface tension dependence on temperature of Duraform polyamide has not been measured. Instead data on PA-12 has been obtained from other published note. These polyamides are the basic material of Duraform polyamide (Nelson, 1998). Table 3 shows A_s and E_s/R obtained for

Duraform polyamide comparing the Duraform behaviour to the known behaviours of Polycarbonate. The values of A_s, E_s/R, A_η, E_η/R, A_σ, E_σ/R used for Polycarbonate.

Table 3: Activation energy and pre-exponential factor for sintering

A_S (1/sec)	E_s/R (K)
20.9e+10	12266.78

4.3. Sintering Rate Formulation

Sintering rate of Duraform polyamide and Protoform composite has been determined to follow equation (4). Activation energy E_s and pre-exponential factor A_s for sintering adopt the values in Table 3. Sintering rate for Duraform polyamide is then written as

$$f = 2.09x10^{11} \exp\left(-\frac{12266.78}{T} - a_x\alpha^b\right) \quad (11)$$

Constants a_x and b are taken as10 and 1 following simulation trials, and α changes gradually from 1 to 0 as the materials heat up through their melting ranges.

4.4. Effect of Pre-exponential Factor A_s

Three values of the pre-exponential factor A_s, as listed together with activation energy in Table 4, have been applied in the simulation to study their effect on the prediction of surface temperature, density and size accuracy of the sintered part. In this table, activation energy E_s, expressed as E_s/R, is kept constant at 12266.8 K for the whole range of A_s.

Table 4: Pre-exponential factor for Duraform polyamide.

	Duraform Polyamide		
E_s/R (K)	12266.8	12266.8	12266.8
A_s (1/sec)	$21x10^{10}$	$25x10^{10}$	$50x10^{10}$

Figure 5 shows the density prediction of sintered part for varying energy densities and compare it with measurement. Here, by increasing the value of pre-exponential factor from 21E+10 to 50E+10 s^{-1}, the slope of the density curve increases considerably. At the same energy density, particularly at the medium and the high energy densities, the increase of A_s by twice also significantly changes the sintered part density prediction. Here, three different values of A_s=21e+10 1/s, 25e+10 1/s and 50e+10 1/s have been applied, while c_2=5.09 and T_b=182 °C are kept constant. This Figure suggests that by setting A_s=50e+10 1/s, the predicted values within the energy density range are in good agreement with the experiment.

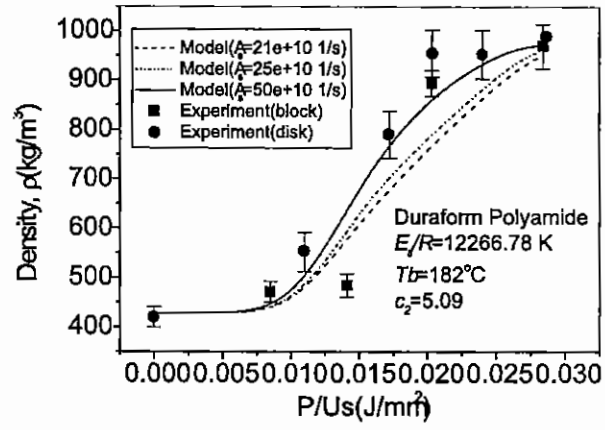

Figure 5. Density validation of Duraform polyamide for various A_s.

5. CONCLUSIONS

A new approach to formulate a sintering law for a crystalline polymer has been developed. The development was conducted on the basis of the existing model for an amorphous polymer. To examine the model prediction, test was carried out to predict density of a sintered part, and it gives a good agreement with the measurement when the pre-exponential factor for sintering (A_s) increases to 50E+10 s^{-1} and keeps the activation energy for sintering (E_s/R) of 12266.78 K.

REFERENCES

Berzins, M., Childs, T.H.C., Dalgarno, K.W., Ryder,G.W., and Stein G., 1995, *Densification and Distortion in Selective Laser Sintering of Polycarbonate Parts*, Solid Freeform Fabrication Symposium, Univer sity of Texas at Austin, 196-203.

Bugeda, G., Cervera, M., and Lombera, G., 1999, *Numerical Prediction of Temperature and Density Distribution in Selective Laser Sintering Process*, Rapid Prototyping Journal, Vol.5, No.1, 21-26.

Carslaw, H.S. and Jaeger, J.C., 1959, *Conduction of Heat in Solids,* 2nd Edition, Oxford University Press, New York, 1-497.

Childs, T.H.C., Cardie, S., and Brown, J.M., 1994, *Selective Laser Sintering of Polycarbonate at Varying Powers, Scan Speeds and Scan Spacings*, Solid Freeform Fabrication Proceedings, University of Texas at Austin, 356-363.

Childs, T.H.C., Ryder, G.R., and Berzins, M., 1997, *Experimental and Theoretical Studies of Selective Laser Sintering*, In Rapid Product Development, Edited by N. Kawa *et al*, Chapman and Hall, 132-141.

Childs, T.H.C., Berzins, M., Ryder, G.R., and Tontowi, A.E., 1999, *Selective Laser Sintering of an Amorphous Polymer-Simulations and Experiments*, Proceedings IMechE, Vol 213, Part B, 333-349.

_____, 1998, *Polyamide-12 for Injection Moulding,* EMS Corporation.

Frenkel, J., 1945, *Viscous Flow of Crystalline Bodies Under the Action of Surface Tension*, Journal of Physics-Academic of Science (USSR), Vol. 9, No.5, 385-391.

Gibson, I. and Shi, D., 1997, *Material Properties and Fabrication Parameters in Selective Laser Sintering Process*, Rapid Prototyping Journal, Vol. 3, No.4, 129-136.

Jaeger, J.C., 1943, *Moving Sources of Heat and The Temperature at Sliding Contacts*, Proceedings of The Royal Society of New south Wales, Vol. 76, Part III, 203-224.

Kohan, M.I., 1995, *Nylon Plastic Handbook*, Carl Hanser Verlag.

Mark, J.E., 1996, *Physical Properties of Polymers Handbook*, American Institute of Physics.

Nelson, J.C., Xue, S., Barlow, J.W., Beaman, J.J., Marcus, H.L., and Bourell, D.L., 1993, *Model of the Selective Laser Sintering of Bisphenol-A Polycarbonate*, Industrial Engineering Chemical Research., Vol. 32, 2305-2317.

Ryder, G.R., Berzins, M., and Childs, T. H.C. , 1996, *Modeling Simple Feature Creation in Selective Laser Sintering*, in Proc 7th Solid Freeform Fabrication Symposium, Austin.

Shimizu, J., Okui, N., and Kikutani, T., 1985, *Simulation of Dynamics and Structure Formation in High Speed Melt Spinning*, Edit. Ziabicki, A. and Kawai, H., Wiley and Sons, New York, 195.

Tszeng, T.C., Im, Y.T., and Kobayashi, S., 1989, *Thermal Analysis of Solidification by The Temperature Recovery Method*, International Journal of Machine Tools Manufacturing, 29-1, 107-120.

Ziabicki, A., Jarecki, L., and Wasiak, A., 1998, *Dynamic Modelling of Melt Spinning*, Computational and Theoretical Polymer Science, Vol. 8, No.1/2, 143-157.